

## First-order valence phase transition in $\text{CeNi}_{1-x}\text{Co}_x\text{Sn}$ alloys

D. T. Adroja and B. D. Rainford

*Department of Physics, Southampton University, Southampton SO17 1BJ, England*

J. M. de Teresa, A. del Moral, and M. R. Ibarra

*Unidad de Magnetismo de Sólidos, Departamento de Física de Materia, Condensada Instituto de Ciencia de Materiales de Aragón, Universidad de Zaragoza del Consejo Superior de Investigaciones Científicas, 50009 Zaragoza, Spain*

K. S. Knight

*ISIS Facility, Rutherford Appleton Laboratories, Chilton, Oxon OX11 0QX, England*

(Received 1 March 1995; revised manuscript received 21 July 1995)

Alloys in the pseudobinary series  $\text{CeNi}_{1-x}\text{Co}_x\text{Sn}$  ( $x=0-0.5$ ) have been investigated using a wide variety of experimental techniques. The gap in the electronic density of states, found in the Kondo compound  $\text{CeNiSn}$  at low temperatures, was found to decrease rapidly with Co concentration. The temperature dependence of the susceptibility shows a dramatic change with Co concentration. In alloys with  $0 \leq x \leq 0.34$ ,  $\chi(T)$  has a form which shows an increasing trend towards intermediate valence behavior with increasing  $x$ : for  $x=0.34$   $\chi(T)$  exhibits a broad maximum at 95 K. For  $x$  in the range 0.35–0.4 the susceptibility exhibits a sharp drop at temperatures between 40 and 75 K (dependent on composition). The unit-cell volume for the  $x=0.38$  alloy, measured by neutron diffraction and linear thermal expansion, shows a 0.3% contraction, and the volume and anisotropic magnetostrictions exhibit large anomalies at the same temperature. We attribute these anomalies to a first-order valence phase transition. Inelastic-neutron-scattering measurements on the  $x=0.38$  alloy above the phase transition temperature  $T_v$  show a quasielastic line and two crystal-field excitations at 26 and 42 meV, while below  $T_v$  the quasielastic peak disappears, and a gap opens up the response, extending up to 20 meV. This type of response is characteristic of intermediate valence systems. All the measurements are consistent with a first-order valence transition, like that observed in the compound  $\text{YbInCu}_4$ .

### I. INTRODUCTION

Among anomalous rare-earth materials displaying intermediate valence or heavy-fermion behavior only a few compounds such as  $\text{SmB}_6$ ,  $\text{SmS}$ ,  $\text{TmSe}$ , and  $\text{YbB}_{12}$  have insulating ground states with a small energy gap at the Fermi level.<sup>1–4</sup> Recently this phenomenon has been discovered for the first time in a number of cerium compounds, in particular  $\text{CeNiSn}$ ,  $\text{Ce}_3\text{Pt}_3\text{Bi}_4$ , and  $\text{CeRhSb}$ .<sup>5–7</sup> It is thought to arise when the Fermi energy lies in the hybridization gap which forms in the electronic density of states at low temperatures, as the system falls into its coherent Fermi-liquid ground state. The gap formation shows up as a rapid rise in the resistivity at low temperatures. This cannot be attributed to simple band-structure effects since the related La, Pr, or Nd compounds show normal metallic behavior down to low temperatures.<sup>8</sup> Compounds of this type are called “Kondo insulators.” Magnetic susceptibility and inelastic-neutron-scattering measurements show that the Ce-based Kondo insulators are intermediate valence materials. X-ray-absorption measurements on  $\text{Ce}_3\text{Pt}_3\text{Bi}_4$  over the temperature range 10–300 K show that the Ce valence varies slowly with temperature.<sup>9</sup> This also is typical of rare-earth compounds displaying intermediate valence behavior.

The work presented here developed out of a systematic study to investigate the effects of chemical pressure, lattice coherence, and hybridization on either the stability of the energy gap at  $E_F$  or the valence state of the Ce ions in the Kondo insulator compounds  $\text{CeNiSn}$  and  $\text{CeRhSb}$ . In our

previous work we have shown that the lattice coherence plays an important role for the stability of the gap rather than the chemical pressure.<sup>10</sup> It was observed that negative chemical pressure (e.g., the substitution of La on the Ce site) and positive chemical pressure (e.g., substitution of Y on the Ce site) have similar effects on the stability of the gap. In order to investigate the effects of hybridization on the stability of the gap and the valence state of Ce ions in  $\text{CeNiSn}$ , without disturbing the lattice coherence of the Ce ions, we have studied alloys in the series  $\text{CeNi}_{1-x}\text{Co}_x\text{Sn}$  ( $x=0$  to 0.5). In a previous paper,<sup>11</sup> we reported a dramatic behavior of the magnetic susceptibility of  $\text{CeNi}_{1-x}\text{Co}_x\text{Sn}$  alloys as a function of Co concentration. In continuation of our investigations on  $\text{CeNi}_{1-x}\text{Co}_x\text{Sn}$  alloys, we present here our results of x-ray diffraction, neutron diffraction, magnetic susceptibility, electrical resistivity, linear thermal expansion, volume, and anisotropic magnetostriction (in fields up to 12 T), and inelastic-neutron-scattering measurements on these alloys. We have found that the transport gap decreases rapidly, and the Ce ion becomes increasingly mixed valent with initial Co content. In the concentration range  $x=0.35-0.4$ , all measurements show highly anomalous behavior in the temperature range between 40 and 80 K (depending on concentration). This behavior is very reminiscent of a first-order valence transition, like that found in the compound  $\text{YbInCu}_4$ .<sup>12</sup> There are only few systems where sharp first-order valence phase transition occurs as a function of temperature at ambient pressure, viz., the  $\gamma$ - $\alpha$  phase transition in cerium metal,  $\text{YbInCu}_4$ , and  $\text{Sm}_{1-x}\text{R}_x\text{S}$ .<sup>12–14</sup> The valence

phase transition is accompanied by a marked drop in magnetic susceptibility and electrical resistivity, anomalies in the thermal expansion and abrupt changes in the unit-cell volume, while maintaining the same crystal symmetry. Besides the  $\gamma$ - $\alpha$  phase transition in Ce metal, the present alloy series  $\text{CeNi}_{1-x}\text{Co}_x\text{Sn}$  ( $x=0.35-0.4$ ) is the only other Ce-based system, so far discovered, to exhibit this remarkable behavior.

## II. EXPERIMENT

Polycrystalline samples of  $\text{CeNi}_{1-x}\text{Co}_x\text{Sn}$  ( $x=0-0.5$ ) were synthesized by arc melting the constituent elements, with purities better than 99.9%, under a high-purity argon atmosphere. The phase purity of the samples was checked using x-ray and neutron powder diffraction. Electrical resistivity measurements were carried out using the standard four probe dc technique. Magnetic susceptibility measurements were made using a vibrational sample magnetometer. Linear thermal expansion and magnetostriction, measured in pulsed and steady fields up to 12 T, were carried out using the strain gauge technique, using four arm bridges. For the magnetostriction measurements unwanted signals were subtracted using a dummy gauge mounted on silica. Neutron-scattering measurements were carried out at the ISIS pulsed neutron facility at the Rutherford Appleton Laboratories, U.K., using the HRPD diffractometer and the HET time-of-flight chopper spectrometer.

## III. RESULTS AND DISCUSSION

### A. X-ray and neutron diffraction

Our analysis of powder x-ray-diffraction and neutron-diffraction data at 300 K on the  $\text{CeNi}_{1-x}\text{Co}_x\text{Sn}$  alloy series revealed that all the samples crystallize in the orthorhombic  $\text{TiNiSi}$ -type structure, and were single phase, except for the  $x=0.5$  sample, which showed the presence of a small amount of a second phase. Our attempt to synthesize  $\text{CeCoSn}$  was not successful. The lattice parameters  $a, b$  increase gradually with increasing Co concentration  $x$ , while the  $c$  parameter decreases with  $x$ . The values of  $a$  and  $c$  are almost equal for the Co concentration near  $x \approx 0.34$ , while for  $x > 0.34$  the value of  $a$  is greater than  $c$ . At room temperature the unit-cell volume  $V_c$  remains almost constant with  $x$ , viz.,  $V_c = 264.406 \text{ \AA}^3$  for  $x=0$  and  $264.386 \text{ \AA}^3$  for  $x=0.4$ .

### B. Resistivity

In order to estimate the transport gap for the  $\text{CeNi}_{1-x}\text{Co}_x\text{Sn}$  alloy series, we measured the temperature dependence of the resistivity between 4.2 and 300 K. The results are shown in Fig. 1(a); the data were measured while heating the samples from the lowest temperature. A rise in the resistivity at low temperatures is evident for  $\text{CeNiSn}$  and the alloy with  $x=0.15$ , which we attribute to the gap formation in the electronic density of states at  $E_F$ . The value of gap energy  $\Delta$  estimated using an activated-type behavior,  $\rho \sim \exp(\Delta/T)$ , is 3 K for  $\text{CeNiSn}$  and 1.1 K for the  $x=0.15$  alloy. No gap-type behavior in the resistivity was observed for alloys with Co concentration  $x \geq 0.25$  between

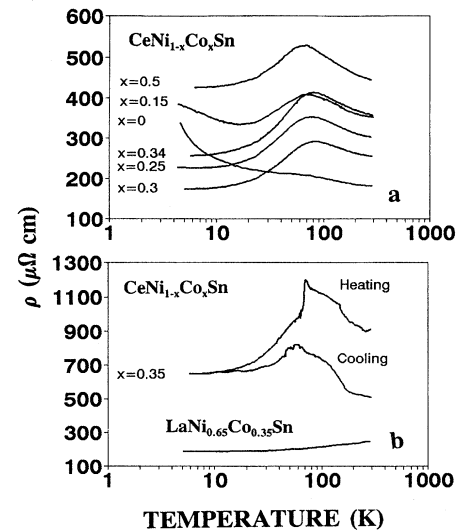


FIG. 1. Resistivity of  $\text{CeNi}_{1-x}\text{Co}_x\text{Sn}$  ( $x=0-0.5$ ) and  $\text{LaNi}_{0.65}\text{Co}_{0.35}\text{Sn}$  alloys as a function of  $\ln(T)$ .

4.2 and 300 K. In the high-temperature regime above 120 K, all the alloys exhibit a  $\ln(T)$  dependence arising from single-ion Kondo behavior. There is a maximum somewhat below 100 K, followed by a drop in the resistivity, attributed to the onset of coherence (for  $\text{CeNiSn}$  this onset of coherence is masked by the opening of the energy gap at  $E_F$  in the low-temperature regime). At higher Co concentrations,  $x=0.35$ , the resistivity exhibits a sharp drop on cooling, and hysteresis on subsequent heating [Fig. 1(b)]. The resistivity behavior for the  $x=0.35$  alloy was the first indication of a first-order valence transition in this alloy. The hysteresis, which leads to a higher room-temperature resistivity after a cooling-heating cycle, is attributed to the opening of microcracks as a result of a first-order volume change (see below). The resistivity of the  $\text{LaNi}_{0.65}\text{Co}_{0.35}\text{Sn}$  alloy, which also crystallized in the  $\text{TiNiSi}$ -type structure, exhibits normal metallic behavior between 4.2 and 300 K [Fig. 1(b)]. The resistivity of  $\text{CeNi}_{1-x}\text{Co}_x\text{Sn}$  with  $x=0.38$  also exhibited an anomalous behavior below 50 K, but the data were not reproducible, due to the large degree of microcracking developed during thermal cycling; therefore these results are not presented here.

### C. Magnetic susceptibility

Figure 2 shows the magnetic susceptibility of  $\text{CeNi}_{1-x}\text{Co}_x\text{Sn}$  alloys ( $x=0-0.5$ ) as a function of temperature between 1.8 and 300 K, measured in applied fields between 0.2 and 0.5 T. The data were collected with increasing temperature. The temperature dependence of the susceptibility is seen to change dramatically as a function of Co concentration. The susceptibility of  $\text{CeNiSn}$  displays Curie-Weiss (CW) behavior between 50 and 300 K with an effective magnetic moment,  $\mu_{\text{eff}} = 2.92 \mu_B$  and paramagnetic Curie temperature  $\theta_p = -196$  K. There is a strong deviation from Curie-Weiss behavior below 50 K. The large negative paramagnetic Curie temperature does not indicate strong antiferromagnetic interactions, but rather crystal-field anisotropy: the susceptibility of single-crystal samples of  $\text{CeNiSn}$

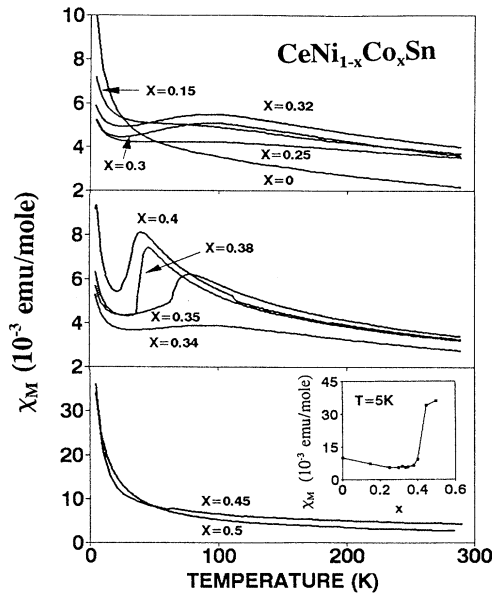


FIG. 2. Magnetic susceptibility of  $\text{CeNi}_{1-x}\text{Co}_x\text{Sn}$  ( $x=0-0.5$ ) alloys as a function of temperature.

is highly anisotropic.<sup>5</sup> This also accounts for the departure from Curie-Weiss behavior at low temperatures. The susceptibility of the alloys with Co concentration  $x=0.15$  and  $0.25$  shows a weak temperature dependence above 25 K. For the alloys with Co concentration between  $x=0.30$  and  $0.34$  the susceptibility develops a broad maximum near 95 K, which is a characteristic feature of Ce-based fluctuating valence systems, e.g.,  $\text{CePd}_3$ . On further increasing the Co concentration a sharp drop in the susceptibility is observed at 75, 47, and 40 K for alloys with Co concentration  $x=0.35$ ,  $0.38$ , and  $0.40$ , respectively. The sharp drop in the susceptibility seen here is similar to that reported in the susceptibility of  $\text{YbInCu}_4$ .<sup>12</sup> We attribute it to a first-order valence transition from a high-temperature, nearly trivalent, state to a low-temperature intermediate valence state of the cerium ion. This attribution has been confirmed from the temperature dependence of the lattice parameters, linear thermal expansion and inelastic-neutron-scattering measurements on the  $x=0.38$  alloy discussed below. The values of  $\mu_{\text{eff}}$  and  $\theta_p$  obtained from the high-temperature Curie-Weiss behavior (data above 100 K) for alloys with Co concentration  $x=0.35$ ,  $0.38$ , and  $0.40$  are  $\mu_{\text{eff}}=3.57\mu_B$ ,  $3.60\mu_B$ ,  $3.57\mu_B$  and  $\theta_p=-182$ ,  $-219$ , and  $-204$  K, respectively. These values for  $\mu_{\text{eff}}$  are higher than that expected for the  $\text{Ce}^{3+}$  ion,  $2.54\mu_B$  and the value  $2.94\mu_B$  observed in  $\text{CeNiSn}$ . This suggests the possibility of a paramagnetic moment on the Co atoms. Our attempt to estimate the moment on the Co atoms in  $\text{LaNi}_{0.65}\text{Co}_{0.35}\text{Sn}$  alloy was not successful due to a small amount of unreacted free Co impurity in this alloy. The susceptibility of the alloys with  $x=0.45$  and  $0.50$  displays normal Curie-Weiss behavior between 50 and 300 K with  $\mu_{\text{eff}}\approx 3\mu_B$  and  $\theta_p\approx -116$  K, strong deviations from CW form below 50 K, and no sign of magnetic ordering down to 1.8 K. The absolute magnitude of the susceptibility at 5 K, shown as an inset in the bottom frame of Fig. 2, decreases

with initial increasing Co concentration, exhibits a minimum between  $x=0.34$  and  $0.38$ , then increases rapidly with higher Co concentration. Heat-capacity measurements on alloys with Co concentrations  $x=0.03$  and  $0.10$  show substantial reductions in the values of  $C/T$  below 30 K.<sup>15</sup> These results are consistent with the theoretical prediction for the Coqblin-Schrieffer model,<sup>16</sup> where in the zero-temperature limit  $\chi(0)\propto\gamma(0)$ . In order to investigate the effect of a high magnetic field on the first-order valence transition, the susceptibility of the  $x=0.40$  Co alloy was measured in an applied field of 4 T. The result shows that the magnetic field does not effect either the valence transition temperature or the sharpness of the transition.

#### D. Neutron-diffraction study of the $\text{CeNi}_{0.62}\text{Co}_{0.38}\text{Sn}$ alloy

Neutron-diffraction measurements were carried out on the  $\text{CeNi}_{0.62}\text{Co}_{0.38}\text{Sn}$  alloy, in order to characterize the first-order phase transition, using the high-resolution powder diffractometer HRPD at the ISIS Facility, Rutherford Appleton Laboratories. Data were collected at a series of temperatures increasing from 4 to 300 K. Accurate values of the lattice parameters were obtained from the analysis of neutron-diffraction patterns collected in the backward angle detector bank, which gives the highest resolution, using the program CAILS (Cell and Integrated Intensity Least Squares) from the Cambridge Crystallography Subroutine Library. The analysis revealed that the observed diffraction patterns over the whole temperature range are consistent with the orthorhombic  $Pnma$  space group. The quality of the fit may be seen from the calculated profile, shown as a solid line in Fig. 3, and the residuals, which are also shown. The temperature dependence of the lattice parameters obtained from the CAILS analysis are shown as a function of temperature in Fig. 4 and the cell volume is plotted in Fig. 5. There is clear evidence of a first-order volume collapse at 45 K (the volume change is 0.3%), without any change of crystal symmetry. The temperature dependence of the  $b$  axis shows a dramatic contraction, while the  $a$ - and  $c$ -axis anomalies are almost the inverse of each other. In the  $\text{TiNiSi}$ -type structure the Ce atoms form a zigzag chain along the  $b$  axis, so the strong contraction along  $b$  axis is likely to be connected with a valence change for the  $4f$  electron through the increasing overlap of the Ce wave functions. There is a region of coexistence of the high-volume and low-volume phases between 30 and 50 K. The intensities of the (301) reflections from the low- and high-volume phases are plotted as a function of temperature in Fig. 6. The estimated percentage of the low-volume phase as a function of temperature is plotted in same the figure (right-hand y axis). Below 35 K almost 100% of the material converts into the low-volume phase. It is interesting to note that for the  $x=0.38$  alloy, out of the six Ni/Co neighbors to a Ce atom, two have shorter bond lengths (3.2025 Å) than the other four (3.2680, 3.3088, two at 3.3148 Å at room temperature). It is possible, therefore, that the Co atoms preferentially occupy these sites. In order to examine this possibility, we attempted a Rietveld profile analysis of the neutron diffraction data, starting from three different space groups, namely  $Pnma$ ,  $Pnm2_1$ , and  $P2_1ma$ . In the latter two cases the space groups are compatible with preferential occupancy of different Ni, Co sites, and the occupancies were allowed

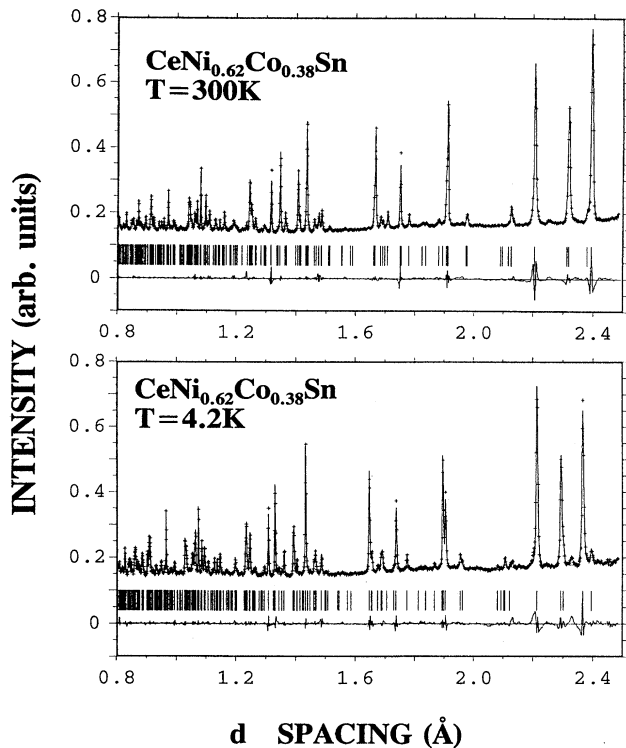


FIG. 3. Neutron-diffraction patterns of  $\text{CeNi}_{0.62}\text{Co}_{0.38}\text{Sn}$  alloy at 300 and 4.2 K, crosses are experimental points, the lines show the calculated profile and the residuals.

to vary in the fitting process. There was no significant difference in the values of  $\chi^2$  and the fitted profiles looked identical. We conclude that, despite the rather large differences in neutron-scattering length between Co and Ni, the data are not sensitive to preferential occupancy of the transition-metal sites.

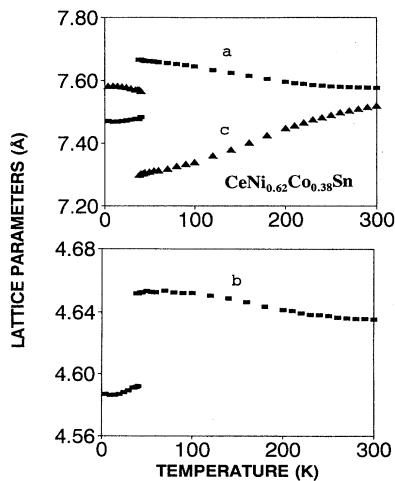


FIG. 4. Lattice parameters  $a$ ,  $b$ , and  $c$  of  $\text{CeNi}_{0.62}\text{Co}_{0.38}\text{Sn}$  alloy as a function of temperature.

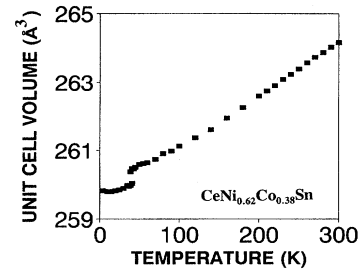


FIG. 5. Unit-cell volume of  $\text{CeNi}_{0.62}\text{Co}_{0.38}\text{Sn}$  alloy as a function of temperature.

### E. Thermal expansion

Figure 7 shows the linear thermal expansion (LTE) for  $\text{CeNi}_{1-x}\text{Co}_x\text{Sn}$  ( $x=0.15, 0.32, \text{ and } 0.38$ ) and  $\text{LaNi}_{0.65}\text{Co}_{0.35}\text{Sn}$  alloys as a function of temperature. The LTE for the alloy with Co concentration  $x=0.38$ , decreases with temperature from 300 K and exhibits a large, abrupt jump at the valence phase transition, with a volume strain  $\Delta V/V \approx 0.36\%$ , in agreement with the volume change observed through the lattice parameters measurements (Fig. 5). The thermal variation of the LTE and the unit-cell volume are very similar. The sharpness of the transition, along with the thermal hysteresis ( $\Delta T = 17$  K) observed in cooling and heating, further support the first-order nature of the valence transition. The LTE for the  $x=0.32$  Co alloy exhibits a linear behavior with temperature between 300 and 80 K. Below 80 K the LTE increases with decreasing temperature, indicating expansion of the lattice. This behavior is unusual for intermediate valence systems, although it has been observed in the fluctuating valence alloys  $\text{Sm}_{1-x}\text{R}_x\text{S}$ .<sup>17</sup> For the alloy with Co concentration  $x=0.15$  the anomalous increase in the LTE at low temperatures disappears, the variation being similar to the LTE observed for the  $\text{LaNi}_{0.65}\text{Co}_{0.35}\text{Sn}$  alloy (Fig. 7). It is to be noted that the thermal expansion measurements made on a second batch of  $\text{CeNi}_{0.62}\text{Co}_{0.38}\text{Sn}$  alloy prepared by a similar method, which exhibited a susceptibility behavior identical to that reported here, showed an extremely large jump in the volume strain  $\Delta V/V = 2.5\%$  at  $T_v$ , while above  $T_v$  the LTE decreased with increasing temperature.

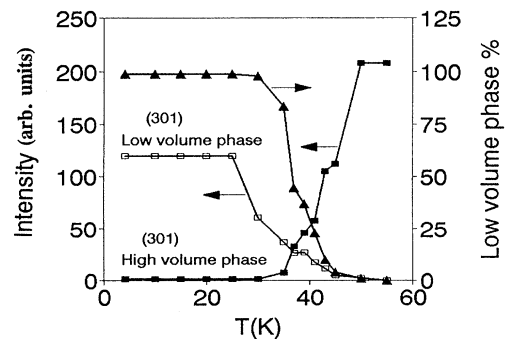


FIG. 6. Intensities of (301) reflections from the low- and high-volume phases and relative percentage of the low-volume phase as a function of temperature.

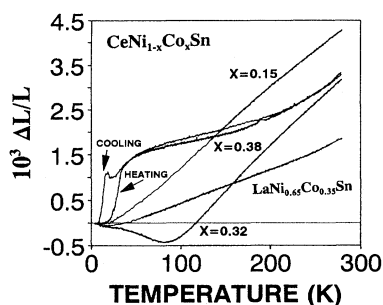


FIG. 7. Linear thermal expansion of  $\text{CeNi}_{1-x}\text{Co}_x\text{Sn}$  ( $x=0.15$ ,  $0.32$ , and  $0.38$ ) and  $\text{LaNi}_{0.65}\text{Co}_{0.35}\text{Sn}$  alloys as a function of temperature.

The overall temperature dependence of the LTE for this alloy is similar to that observed for  $b$  the axis in neutron-diffraction measurements (Fig. 4). The origin of this behavior may result from strongly preferred orientation in this sample.

#### F. Magnetostriction

Magnetostriction measurements were made on  $\text{CeNi}_{0.62}\text{Co}_{0.38}\text{Sn}$  in fields up to 12 T, using a superconducting solenoid, for both parallel ( $\lambda_{\parallel}$ ) and perpendicular ( $\lambda_{\perp}$ ) geometry, across the temperature range 5–100 K. The technique allowed  $\lambda_{\parallel}$  and  $\lambda_{\perp}$  to be measured simultaneously via two strain gauges mounted on the sample, parallel and perpendicular to the applied magnetic field. The thermal expansion was also measured with the same arrangement. In Figs. 8 and 9, we show  $\lambda_{\parallel}$  and  $\lambda_{\perp}$  measured at the highest field (12 T) together with the linear thermal expansion coefficient  $\alpha=(1/L)(\Delta L/\Delta T)$ . Both  $\lambda_{\parallel}$  and  $\lambda_{\perp}$  have peaks near 32.5 K, at the same temperature as the peak in the thermal expansion. Isotherms of  $\lambda_{\parallel}$  and  $\lambda_{\perp}$  with increasing and decreasing field are shown in Fig. 10, at a temperature of 32.5 K. A large hysteresis is observed, confirming that the field-induced transition has first-order character. The different values  $\lambda_{\parallel}$  and  $\lambda_{\perp}$  at the maximum field may be due to the presence of microcracks within the part of the sample in contact with the active region of the strain gauges. The magnetostriction of another  $\text{CeNi}_{0.62}\text{Co}_{0.38}\text{Sn}$  sample was measured previously

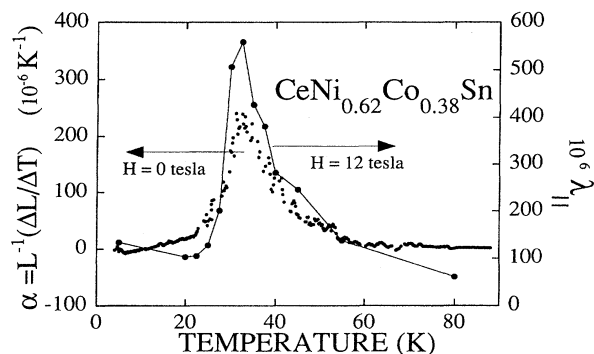


FIG. 8. Parallel magnetostriction ( $\lambda_{\parallel}$ ) and thermal expansion coefficient of  $\text{CeNi}_{0.62}\text{Co}_{0.38}\text{Sn}$  as a function of temperature.

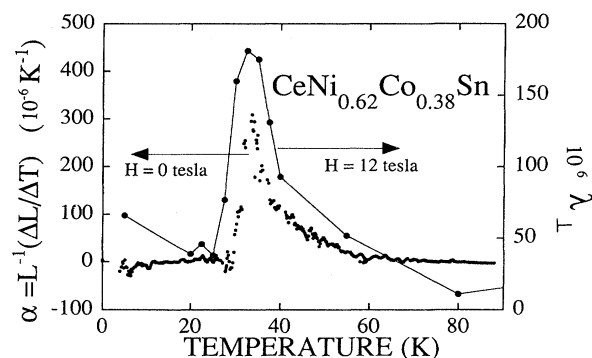


FIG. 9. Perpendicular magnetostriction ( $\lambda_{\perp}$ ) at 12 T and thermal expansion coefficient of  $\text{CeNi}_{0.62}\text{Co}_{0.38}\text{Sn}$ , as a function of temperature.

with pulsed magnetic fields.<sup>18</sup> These measurements gave the same maximum value for  $\lambda_{\parallel}$  and  $\lambda_{\perp}$  at the peak, but, rather surprisingly, the peaks in  $\lambda_{\parallel}$  and  $\lambda_{\perp}$  occurred at *different* temperatures, 27 and 45 K, respectively. We note here that the pulsed field method did not allow  $\lambda_{\parallel}$  and  $\lambda_{\perp}$  to be measured simultaneously, so it is likely that the difference in the peak temperatures arose from the temperature cycling of the sample through the first-order transition. The magnetostriction of the alloy  $\text{LaNi}_{0.65}\text{Co}_{0.35}\text{Sn}$  was also measured for comparison: this showed no anomaly and had a small magnitude, below 100 microstrains, confirming that the effects in the cerium alloy are related to the properties of the cerium ion, and not to the Co(Ni) transition-metal atoms. We attribute the large anomaly in the cerium alloy to the volume difference between the low-temperature and high-temperature states. In the vicinity of the transition tempera-

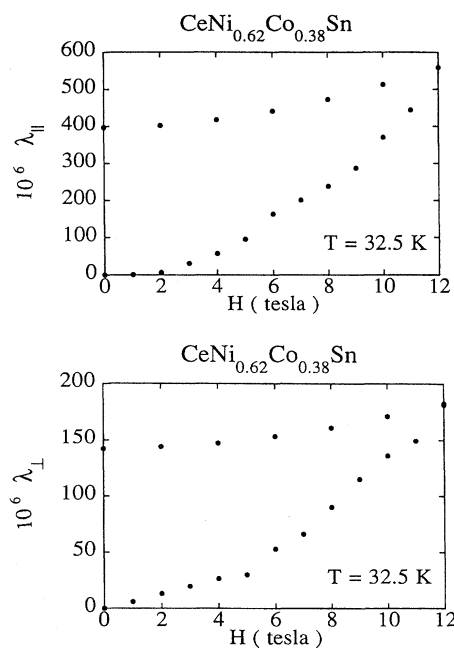


FIG. 10. Parallel ( $\lambda_{\parallel}$ ) and perpendicular ( $\lambda_{\perp}$ ) magnetostriction of  $\text{CeNi}_{0.62}\text{Co}_{0.38}\text{Sn}$  as a function of field at 32.5 K.

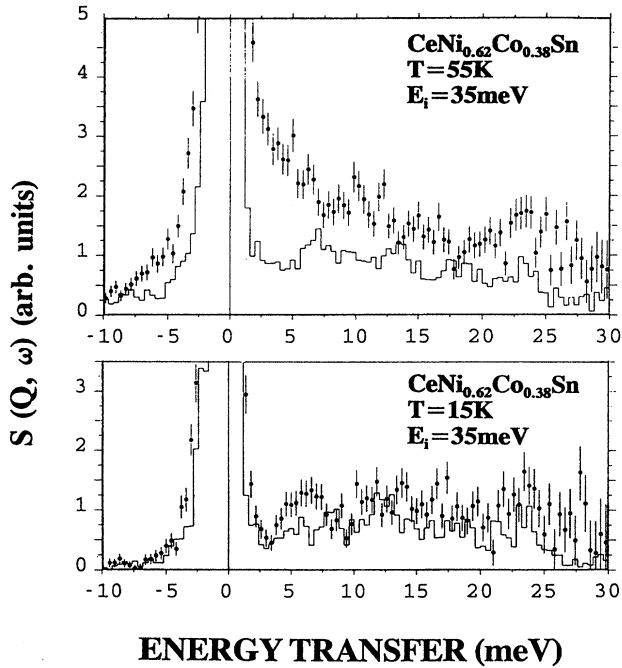


FIG. 11. Inelastic-neutron-scattering spectra from the alloy  $\text{CeNi}_{0.62}\text{Co}_{0.38}\text{Sn}$  at 55 and 15 K with incident energy  $E_i = 35$  meV; the histogram represents the phonon contribution, estimated by scaling spectra from a high-angle detector bank.

ture a 12-T field is able to transform part of the sample from the low-volume state to the more magnetic high-volume state. Below the transition temperature, it should be possible to transform the sample completely with a large enough magnetic field. This has been shown already for  $\text{YbInCu}_4$ .<sup>19</sup>

### G. Inelastic neutron scattering

Inelastic-neutron-scattering measurements were carried out on the  $\text{CeNi}_{0.62}\text{Co}_{0.38}\text{Sn}$  alloy, using the HET chopper spectrometer at ISIS, with the aim of studying the dynamical magnetic response through the first-order valence transition. Spectra were collected with incident neutron energies ( $E_i$ ) of 35 and 60 meV at temperatures of 15 and 55 K. The data are shown in Fig. 11 ( $E_i = 35$  meV) and Fig. 12 ( $E_i = 60$  meV). Estimates of the phonon scattering are plotted as histograms in these figures. These estimates were obtained by scaling the spectra from the high-angle ( $118^\circ$ ) detector bank. At high scattering angles the magnetic form factor has dropped to a very low value and the magnetic contribution to the scattering is negligible. The scaling factor was obtained by using the ratio of intensities in the high- and low-angle detector banks from measurements (Fig. 15) on the isostructural alloy  $\text{LaNi}_{0.65}\text{Co}_{0.35}\text{Sn}$ , using the method outlined in the Appendix. Figures 13 and 14 show the difference spectra (total scattering minus phonon scattering), representing the magnetic response above and below the valence transition for incident neutron energies of 35 and 60 meV, respectively. It is clear that the form of the magnetic scattering is quite different above and below the valence transition. At 55 K the mag-

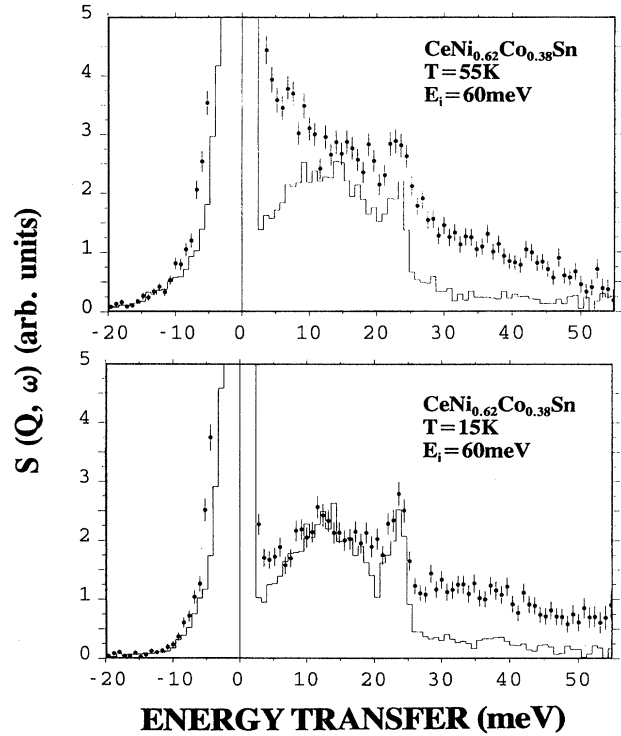


FIG. 12. Inelastic-neutron-scattering spectra from the alloy  $\text{CeNi}_{0.62}\text{Co}_{0.38}\text{Sn}$  at 55 and 15 K with incident energy  $E_i = 60$  meV; the histogram represents the phonon contribution, estimated by scaling spectra from a high-angle detector bank.

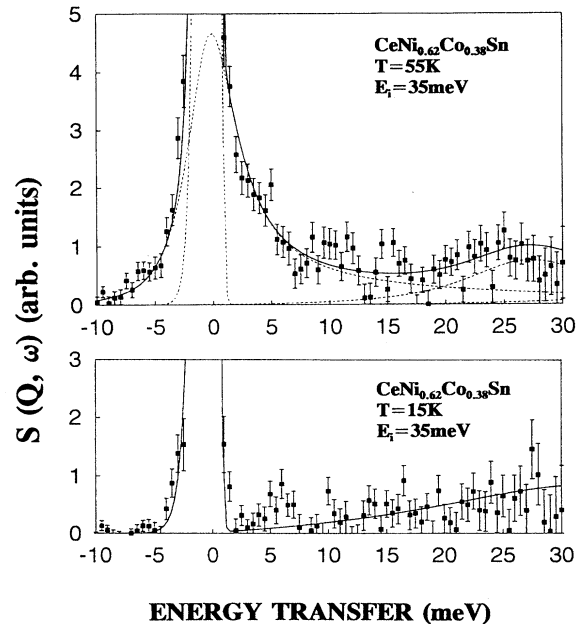


FIG. 13. Magnetic scattering (total scattering minus phonon) for  $\text{CeNi}_{0.62}\text{Co}_{0.38}\text{Sn}$  at 55 and 15 K for incident energy 35 meV; the solid line represents the fit (see text).

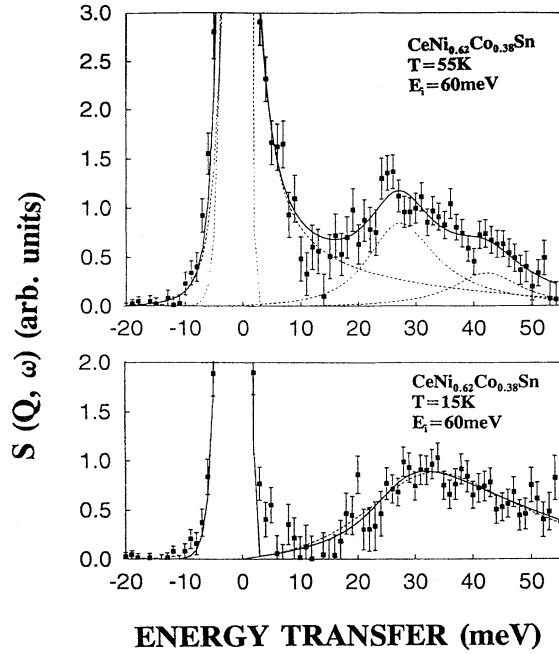


FIG. 14. Magnetic scattering (total scattering minus phonon) for  $\text{CeNi}_{0.62}\text{Co}_{0.38}\text{Sn}$  at 55 and 15 K for incident energy 60 meV; the solid line represents the fit (see text).

netic signal consists of a quasielastic response centered at zero energy transfer and two broadened inelastic peaks centered near 26 and 42 meV. This form of the scattering is consistent with the response expected from trivalent cerium, in which the  $J = \frac{5}{2}$  multiplet has been split into three doublets by the crystal field. The quasielastic response arises from scattering within the doublets, while the inelastic peaks are attributed to two unresolved crystal-field excitations, broadened by spin-lattice relaxation (dominantly the  $4f$ -conduction electron interaction) and also by the site disorder. Below the valence transition, at 15 K, both the quasielastic peak and the crystal-field excitations disappear, leaving a broad inelastic response, with an energy gap extending up to 15 meV. This is characteristic of the response found in intermediate valence materials, such as  $\text{YbAl}_3$ ,<sup>20</sup> and the low-volume state of  $\text{YbInCu}_4$ .<sup>21</sup> Indeed the overall behavior of the inelastic neutron scattering is very similar to that found in  $\text{YbInCu}_4$ ,<sup>21</sup> where at high temperatures broadened crystal-field excitations are found, while below the first-order valence transition the response appears as a broad inelastic peak centered on 40 meV, with a gap of order 20 meV. The magnetic spectra at 55 K were fitted to a line-shape profile consisting of a quasielastic Lorentzian curve, plus two inelastic Lorentzians (solid lines, Figs. 13 and 14). The fitted quasielastic linewidth was  $\Gamma/2 = 2.2 \pm 0.2$  meV, while the inelastic peaks were centered at 26.5 and 42.1 meV, with linewidths of 7.3 meV. The inelastic response at 15 K was fitted to an inelastic Lorentzian curve (dashed line in Fig. 14) and also to the Kuramoto-Muller-Hartmann (KMH) spectral function<sup>22</sup> (solid line in Fig. 14). The latter takes the form

$$\text{Im}\chi(\omega) = \frac{C\alpha\omega}{u^2(u^2 + 4\alpha^2)} \left\{ \alpha \ln[(1-u^2)^2 + 4u^2\alpha^2] + |u| \left[ \frac{\pi}{2} - \tan^{-1} \left( \frac{1-u^2}{2|u|\alpha} \right) \right] \right\},$$

where  $u = \omega/\omega_0$  and  $\alpha = \sin(\pi\langle n_f \rangle/N)$ . Here  $\omega_0$  represents the characteristic Kondo energy,  $\langle n_f \rangle$  the occupancy of the  $4f$  level and  $N$  the degeneracy of the  $4f$  state. The fitted parameters were  $\omega_0 = 26.5$  meV and  $\alpha = 0.29$ . It can be seen that there is very little difference between the KMH spectral function and an inelastic Lorentzian line shape. In neither case does the line shape give a clear gap in the response, as the data appear to require. The value of  $\omega_0$  implies a Kondo temperature of order 300 K. If we assume  $\langle n_f \rangle \approx 1$  the value of  $\alpha$  corresponds to a degeneracy  $N$  of 10.6, which lies between that of the Hund's rule ground state ( $N = 6$ ) and the full degeneracy ( $N = 14$ ) expected for a  $4f^1$  state (i.e., neglecting spin-orbit coupling). It is not clear that this is physically meaningful, since the KMH theory is only established in the single-impurity case.

#### IV. CONCLUSIONS

The alloys series  $\text{CeNi}_{1-x}\text{Co}_x\text{Sn}$  has been investigated by six different experimental techniques, all of which confirm that in the Co concentration range  $x = 0.35 - 0.40$  there is a first-order valence phase transition at temperatures between 40 and 80 K (depending on concentration), from a high temperature, nearly trivalent, state to a low-temperature intermediate valence state of the cerium ions. The alloys with Co concentration  $x = 0.15 - 0.34$  exhibit classical valence fluctuation behavior, indicating strong hybridization between the  $4f$  electrons and the conduction electrons. Alloys with  $x$  greater than 0.40 show a Curie-Weiss susceptibility, as expected for  $\text{Ce}^{3+}$  ion in the presence of the crystalline electric field, although the Curie constants are enhanced compared to the value expected for trivalent cerium. The measurements we have made so far cannot establish whether there is a small moment on the Co(Ni) sites. Measurements of the local susceptibility at the Ce or Co(Ni) sites with a microscopic probe [e.g., time differential perturbed angular correlation (TDPAC) for the  $^{140}\text{Ce}$ , Co NMR] would be useful to understand fully the character of the magnetic moment as a function of either temperature or Co concentration. The valence transition temperature and the temperature dependence of the susceptibility depend strongly on the Co concentration, which suggest in particular a large change in the electronic density of state with Co concentration. Susceptibility measured in an applied field of 4 T shows that the valence transition is not sensitive to the magnetic field. We have observed that, in alloys showing the first-order valence transition, the parallel ( $\lambda_{\parallel}$ ) and perpendicular ( $\lambda_{\perp}$ ) magnetostriction exhibit peaks at  $T_v$ . The change in character of the inelastic neutron cross section through the valence transition is quite distinctive. Below  $T_v$  a gap opens up in the response, and all the spectral weight below about 15 meV disappears. This change can clearly account for the drop in the bulk susceptibility, though a detailed comparison has not been attempted since the neutron data were not placed on an

absolute scale. The parallels with the neutron-scattering data for  $\text{YbInCu}_4$  are very clear.

It is not yet clear why the first-order valence transition occurs in this particular alloy series in such a narrow range of composition. In the  $\text{Yb}_{1-x}\text{In}_x\text{Cu}_2$  system the valence transition appears to be associated with chemical ordering on the Yb/In sublattice, since the susceptibility anomalies are clearest in well-annealed samples which are ordered, as  $\text{YbInCu}_4$ , into the C15b structure.<sup>12,21</sup> For the  $\text{CeNi}_{1-x}\text{Co}_x\text{Sn}$  system we note that the valence transition occurs in a concentration range near  $\text{Ce}_3\text{Ni}_2\text{CoSn}_3$ , that the  $a$  and  $c$  lattice parameters are almost equal (pseudotetragonal unit cell), and that two of the Ce-(Ni/Co) nearest-neighbor bond lengths are shorter than the other four. However, profile analysis of the neutron-diffraction patterns failed to give evidence of ordering of the transition-metal atoms in a superlattice structure. Further work in this area, e.g., a single-crystal neutron-diffraction study, would be useful.

#### APPENDIX: ESTIMATION OF THE PHONON SCATTERING IN THE INELASTIC-NEUTRON-SCATTERING DATA

Extensive Monte Carlo simulations by Osborn (private communication) and ourselves have shown that the form of the phonon scattering from a slab-shaped polycrystalline sample takes the form

$$S(Q, \omega) = A(\omega) + B(\omega)Q^2, \quad (\text{A1})$$

where  $B(\omega)$  results from single-scattering processes, while  $A(\omega)$  represents multiple-scattering processes, which are found to be isotropic to a very good approximation. In the present case we have used inelastic-neutron-scattering measurements on the alloy  $\text{LaNi}_{0.65}\text{Co}_{0.35}\text{Sn}$  as a way of checking the predicted form in (A1), by scaling the normalized high angle (large  $Q$ ) data by a numerical factor and comparing this with the scattering measured at low angles (small  $Q$ ). At large  $Q$  the single scattering  $B(\omega)$  term will domi-

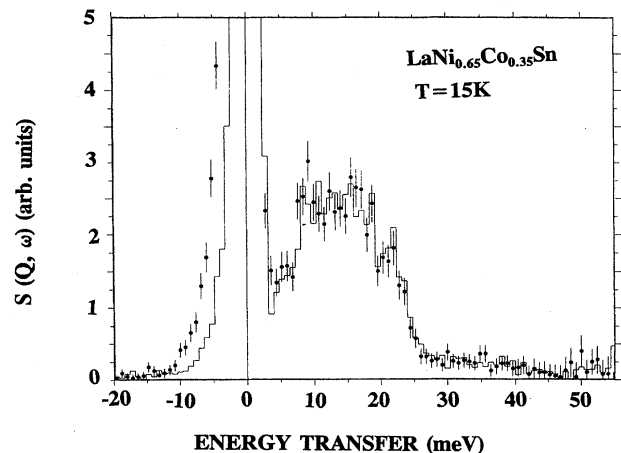


FIG. 15. Phonon scattering from  $\text{LaNi}_{0.65}\text{Co}_{0.35}\text{Sn}$ ; symbols, low-angle data; histogram, high-angle data scaled by a numerical factor.

nate, while at small  $Q$  the phonon scattering is due entirely to the multiple-scattering term  $A(\omega)$ . The low-angle data and scaled high-angle data are plotted together in Fig. 15, where it can be seen that they superimpose almost perfectly. Inelastic-neutron-scattering spectra of  $\text{LaNi}_{0.65}\text{Co}_{0.35}\text{Sn}$  with incident energy ( $E_i$ ) of 35 meV also show a scaling behavior similar to that of 60 meV (figure not shown here). This means that the energy dependence of  $A(\omega)$  and  $B(\omega)$  are very similar. We now assume that the same is true for the phonons in the  $\text{CeNi}_{0.62}\text{Co}_{0.38}\text{Sn}$  alloy: this is very likely, since the only difference between the Ce and La alloys is the small atomic mass difference between Ce and La. We have used exactly the same numerical scaling factor which gives the superposition in Fig. 15 to scale the high-angle data for the Ce alloy, as a means of extrapolating the phonon scattering from large  $Q$  to small  $Q$ . The resulting spectra are shown as histograms in Figs. 11 and 12.

- <sup>1</sup> See, for example, T. Kasuya, *Jpn. J. Appl. Phys.* **8**, 3 (1993); A. Jayaraman *et al.*, *Phys. Rev. Lett.* **25**, 1430 (1970).
- <sup>2</sup> J. M. Robinson, *Phys. Rev. Lett.* **51**, 1 (1979).
- <sup>3</sup> P. Haen *et al.*, *Phys. Rev. Lett.* **43**, 304 (1979).
- <sup>4</sup> T. Kasuya, *J. Less Common Met.* **127**, 337 (1987).
- <sup>5</sup> T. Takabatake, F. Teshima, H. Fujii, S. Nishigori, T. Suzuki, T. Fujita, Y. Yamaguchi, J. Sakurai, and D. Jaccard, *Phys. Rev. B* **41**, 9607 (1990).
- <sup>6</sup> M. F. Hunley, P. C. Canfield, J. D. Thompson, and Z. Fisk, *Phys. Rev. B* **42**, 6842 (1990).
- <sup>7</sup> S. K. Malik and D. T. Adroja, *Phys. Rev. B* **43**, 6277 (1991).
- <sup>8</sup> D. T. Adroja, Ph.D. thesis, Indian Institute of Technology, Bombay, India, 1990 (unpublished).
- <sup>9</sup> G. H. Kwei, J. M. Lawrence, and P. C. Canfield, *Phys. Rev. B* **49**, 14 708 (1994).
- <sup>10</sup> D. T. Adroja and B. D. Rainford, *J. Magn. Magn. Mater.* **135**, 333 (1994).
- <sup>11</sup> D. T. Adroja and B. D. Rainford, *Physica B* **199&200**, 498 (1994).
- <sup>12</sup> I. Felner and I. Nowik, *Phys. Rev. B* **33**, 617 (1986).
- <sup>13</sup> K. A. Gschneidner, Jr., R. O. Elliot, and R. R. McDonald, *J. Phys. Chem. Solids* **23**, 1191 (1962).
- <sup>14</sup> A. Jayaraman, P. Dernier, and L. D. Longinotti, *High Temp. High Pressure* **7**, 1 (1975).
- <sup>15</sup> T. Takabatake, G. Nakamoto, H. Tanaka, Y. Banso, H. Fujii, S. Nishigori, H. Goshima, T. Suzuki, T. Fujita, I. Oguro, T. Hiraoka, and S. K. Malik, *Physica B* **199&200**, 457 (1994).
- <sup>16</sup> B. Coqblin and J. Schrieffer, *Phys. Rev.* **185**, 847 (1969); V. T. Rajan, *Phys. Rev. Lett.* **51**, 308 (1991).
- <sup>17</sup> A. Jayaraman, in *Handbook on the Physics and Chemistry of Rare Earths*, edited by K. A. Gschneidner, Jr. and L. R. Eyring (North-Holland, Amsterdam, 1979), Vol. 2, p. 575.
- <sup>18</sup> D. T. Adroja, D. del Moral, J. M. de Teresa, M. R. Ibarra, and B. D. Rainford, *J. Magn. Magn. Mater.* **140-144**, 1219 (1995).
- <sup>19</sup> K. Yoshimori, T. Nitta, M. Mekata, T. Shimizu, T. Sakakibara, T. Goto, and G. Kodo, *Phys. Rev. Lett.* **60**, 9 (1988).
- <sup>20</sup> A. P. Murani, *Phys. Rev. B* **50**, 9882 (1994).
- <sup>21</sup> A. Severing, E. Gratz, B. D. Rainford, and K. Yoshimura, *Physica B* **163**, 409 (1990).
- <sup>22</sup> Y. Kuramoto and E. Müller-Hartmann, *J. Magn. Magn. Mater.* **52**, 122 (1985).